Small-tunneling-amplitude boson-Hubbard dimer. II. Dynamics

G. Kalosakas and A. R. Bishop
Theoretical Division and Center for Nonlinear Studies, Los Alamos National Laboratory, Los Alamos, New Mexico 87545

V. M. Kenkre
Center for Advanced Studies and Department of Physics and Astronomy, University of New Mexico, Albuquerque, New Mexico 87131
(Received 9 October 2002; published 11 August 2003)

We present analytical relations for the quantum evolution of the number difference of bosons between the two sites of a double-well potential, by using perturbative results for small tunneling amplitudes in the two-mode approximation. Results are obtained for two different initial conditions: completely localized states and coherent spin states. In the former case both the short and the long time behavior is investigated and the characteristic Bohr frequencies of the energy spectrum are determined. In the latter case we calculate the short time-scale evolution of the number difference. The analytical expressions compare favorably with direct numerical solutions of the quantum problem. Finally, we discuss the corresponding Gross-Pitaevskii (i.e., mean-field) dynamics and we point out the differences between the full quantum evolution and the mean-field evolution.

DOI: 10.1103/PhysRevA.68.023602 PACS number(s): 03.75.Kk, 05.30.Jp

I. INTRODUCTION

There are few examples in physics where analytical insight of the complex dynamics displayed by a many-body quantum system can be gained. Even if such an analytical description is limited to a region of the parameter space, it is important for understating some aspects of quantum evolution. For example, it allows us to observe what are the quantum effects in the solutions determined by approximation schemes, such as commonly used mean-field theories. This issue is particularly timely as regards the dynamics of a Bose-Einstein condensate (BEC).

The Gross-Pitaevskii equation [1,2] constitutes a mean-field approximation—derived through a generalization of the Bogoliubov perturbation theory developed for superfluid ^{4}He—for the time-dependent behavior of the macroscopic wave function of a BEC. This equation has been able to efficiently describe the experimental observations followed by the first realizations of Bose-Einstein condensation in dilute alkali vapors [3], as well as solitons created by employing delicate phase engineering in such systems [4]. However, recently, an increasing interest has been stimulated for exploring quantum effects beyond the mean-field approximation. This trend is reinforced by the appearance of experiments that study phenomena that cannot be described by the Gross-Pitaevskii equation [5,6].

In this study we derive analytical results for the quantum dynamics of a simple many-body system [see Hamiltonian (2) below] consisting of two weakly coupled bosonic traps, taking into account particle-particle interactions. This system can describe, in a perturbative limit, a BEC confined in a double-well potential, where the atoms can tunnel between the two minima of the trap. In addition to several theoretical studies [7–11], such a situation has also been experimentally realized [12]. The same system can also describe two coupled intramolecular stretching modes [13–15]. Finally, a related problem is the case of two BECs in a different hyperfine state, confined in the same magnetic trap and coupled through a weak driving field [16,17].

The many-body Hamiltonian describing a dilute gas of N interacting bosons in an external double-well potential V_{dw} is

$$\mathcal{H}=\int d^3r\left[\hat{\Psi}^\dagger(\vec{r})\left(-\frac{\hbar^2}{2m}\nabla^2\right)\hat{\Psi}(\vec{r})+V_{dw}\hat{\Psi}^\dagger(\vec{r})\hat{\Psi}(\vec{r})+\frac{2\pi\hbar^2 a}{m}\hat{\Psi}^\dagger(\vec{r})\hat{\Psi}^\dagger(\vec{r})\hat{\Psi}(\vec{r})\hat{\Psi}(\vec{r})\right], \quad (1)$$

where $\hat{\Psi}^\dagger(\vec{r})$ and $\hat{\Psi}(\vec{r})$ are bosonic field operators creating and annihilating, respectively, atoms at the position $\vec{r}$, and we have used that, for a dilute and cold gas, the two-body interaction $V(\vec{r}-\vec{r}')$ can be substituted by $(4\pi\hbar^2 a/m)\delta(\vec{r}-\vec{r}')$, with a the s-wave scattering length and m the atomic mass.

In the following section we present the so-called two-mode approximation, which drastically simplifies the Hamiltonian (1). Then we briefly recall the structure of the energy spectrum for small tunneling amplitudes, as has been obtained in a previous paper [11] by using perturbation theory. In the following sections we apply the perturbative results for the stationary states presented in Ref. [11], in order to estimate the time evolution of the mean value of the population difference in the two wells of the potential. We consider two different initial conditions, viz., completely localized states (Sec. III) and coherent spin states (Sec. IV). The corresponding numerical solutions of the time-dependent Schrödinger equation are also presented and the quantum results are compared with the predictions of the mean-field (Gross-Pitaevskii) dynamics. In Sec. V we draw our conclusions.

II. THE BOSON-HUBBARD DIMER

When the separation of the two wells is sufficiently large that the overlap of the corresponding single-atom ground states at each well is very small, a first-order perturbative

approximation can be applied, which leads to a significant simplification of the problem; the infinite dimensional Hilbert space of Hamiltonian (1) is reduced to a finite-dimensional system.

A. Two-mode approximation

The two-mode approximation is described in detail in Ref. [7] and is valid when the two lowest eigenenergies of a single boson subjected to the double-well potential are close together and well separated from the other energy eigenvalues. It consists of an expansion of the field operators of Eq. (1) in terms of the weakly overlapped single-atom ground states at each well of the potential. Then, retaining first-order terms in the Hamiltonian with respect to the small overlap, yields the ''boson-Hubbard'' dimer Hamiltonian, which in dimensionless form is

$$H=-k(b_1^\dagger b_2+b_2^\dagger b_1)+(b_1^\dagger b_1^\dagger b_1 b_1+b_2^\dagger b_2^\dagger b_2 b_2). \quad (2)$$

In this expression the dimensionless parameter k is the tunneling amplitude between the two wells in units of the atom-atom interaction energy U, which defines the unit of energy. The operators $b_i^\dagger$ (b_i), $i=1,2$, create (annihilate) bosons at the ith well. For the connection of the quantities appearing in Eq. (2) with the microscopic parameters of Eq. (1), see Eqs. (2) and (3) of Ref. [11], or Ref. [7]. We mention that parameter k can be tuned over several orders of magnitude, by varying either the height of the barrier between the minima of the double well or the scattering length through a Feshbach resonance [18,19].

The two-mode approximation assumes that the atom-atom interactions do not significantly affect the ground state properties of the two individual wells. This means that the number of bosons in the condensate should not be larger than a few thousands [see Eq. (13) of Ref. [7]].

B. Angular momentum representation

A useful transformation can be performed from the operators b_i and $b_i^\dagger$ to angular momentum operators, yielding an equivalent representation of Eq. (2) [7,9,11]:

$$H=-2kJ_x+2J_z^2. \quad (3)$$

The dimensionless total angular momentum J (in units of $\hbar$) is conserved by this Hamiltonian and the corresponding quantum number is

$$j=\frac{N}{2}\Rightarrow J^2=\frac{N}{2}\left(\frac{N}{2}+1\right). \quad (4)$$

The dimensionality of the relevant Hilbert space is equal to $2j+1=N+1$ and depends on the fixed number of bosons. The z component of angular momentum provides the atom number difference between the two wells:

$$J_z=\frac{N_2-N_1}{2}, \quad (5)$$

where N_1 (N_2) gives the number of bosons at the $i=1$ $(i=2)$ well. The relative number difference is given by

$$\frac{N_2-N_1}{N}=\frac{\langle J_z\rangle}{N/2}. \quad (6)$$

C. Structure of the energy spectrum for small tunneling amplitude

For $k=0$ the $N+1$ eigenvalues of the Hamiltonian (3) form degenerate pairs of levels with energies

$$E_{m^\pm}^{(0)}=2m^2, \quad m=\frac{1}{2} \text{ or } 1,\ldots,\frac{N}{2}-1,\frac{N}{2}, \quad (7)$$

where m is a positive integer or half integer depending on whether N is even or odd, respectively. The corresponding eigenvectors are

$$|h_{m^\pm}^{(0)}\rangle=|m^\pm\rangle=\frac{1}{\sqrt{2}}(|m\rangle\pm|-m\rangle), \quad (8)$$

where $|\pm m\rangle$ are the eigenvectors of J_z: $J_z|\pm m\rangle=\pm m|\pm m\rangle$. For an even number of bosons the ground state $|h_0^{(0)}\rangle=|0\rangle$ is nondegenerate with eigenvalue $E_{m=0}^{(0)}=0$.

As k increases from zero the degeneracy is gradually lifted, starting from the lower levels, i.e., the smaller m. This means that for a fixed value of k, the splitting $\Delta E_{m^\pm}=|E_{m^+}-E_{m^-}|$ decreases with m. Up to second order in k the perturbative energy eigenvalues are given by [11]

$$E_{m^\pm}^{(2)}=2m^2+k^2\frac{J^2+m^2}{4m^2-1} \quad \text{for} \quad m\neq 1,\frac{1}{2}, \quad (9)$$

$$E_{1/2^\pm}^{(2)}=\frac{1}{2}\mp k\sqrt{J^2+\frac{1}{4}}-\frac{k^2}{4}\left(J^2-\frac{3}{4}\right) \quad \text{for odd } N, \quad (10)$$

and

$$E_{1^\pm}^{(2)}=2+\frac{k^2}{6}(2J^2\pm 3J^2+2) \quad \text{for even } N, \quad (11)$$

where J^2 is given by Eq. (4). From now on, for simplicity and compact notation, we use expressions or summations with index $m^\pm$ referring also to the level $m=0$ (for even N), as in Eq. (9). In these cases, instead of two levels $0^\pm$, we mean the single level 0.

The splittings $\Delta E_{m^\pm}$ of the levels $E_{m^\pm}$ for $m>1$, which are still degenerate up to second order, Eq. (9), are of the order k^{2m} and have been analytically calculated elsewhere [see Eq. (7) of Ref. [20]]. Consequently, the higher energy levels form quasidegenerate pairs for relatively small k. The particular value of k up to which these levels could be still considered quasidegenerate depends on N and the specific level $E_{m^\pm}$ [11].

The corresponding perturbative corrections in the eigenvectors of Eq. (8) contain the $|(m\pm 1)^\pm\rangle$ at first order and $|(m\pm 2)^\pm\rangle$ at second order, except for the cases where m

$+1$ or $m+2$ is larger than $N/2$ and $m-1$ or $m-2$ is negative. For the exact expressions see Sec. III B of Ref. [11]. The corrections preserve the symmetry of the unperturbed eigenvector, i.e., the corrections of $|h_{m^+}\rangle$ ($|h_{m^-}\rangle$) contain $|(m\pm1)^+\rangle$, $|(m\pm2)^+\rangle$($|(m\pm1)^-\rangle$, $|(m\pm2)^-\rangle$), with $|0\rangle$ belonging to the even parity symmetry class of $|m^+\rangle$.

D. Time evolution of the relative number difference

In the following two sections we use the analytical results of the energy eigenstates [11] in order to calculate the time evolution of the mean value of J_z, i.e., the bosons number difference at the two sites of the dimer apart from a factor of 2. The mean value is given by the standard relation [21]

$$\langle J_z(\tau)\rangle = \sum_{n=m^\pm} \sum_{n'=m^\pm} \phi_n^\star \phi_{n'} \langle h_n|J_z|h_{n'}\rangle e^{i(E_n-E_{n'})\tau}, \tag{12}$$

where the dimensionless time is $\tau=(U/\hbar)t$. All the frequencies ω hereafter represent dimensionless frequencies (in units of $U/\hbar$). The sums of n,n' in the last expression are over all the energy stationary states $|h_{m^\pm}\rangle$, for $m=0$ or 1/2, . . . ,$N/2$, and ϕ_n are the projections of the initial condition $|\Psi(0)\rangle$ on the basis of $|h_{m^\pm}\rangle$, i.e.,

$$|\Psi(0)\rangle = \sum_{n=m^\pm} \phi_n |h_n\rangle. \tag{13}$$

The analytical perturbative results for the eigenfunctions make possible the calculation of the corresponding weights $\phi_n^\star \phi_{n'} \langle h_n|J_z|h_{n'}\rangle$ with which the Bohr frequencies of the spectrum, $E_n-E_{n'}$, contribute to the quantum evolution of Eq. (12). The matrix elements $\langle h_n|J_z|h_{n'}\rangle$ for $n'=n,n\pm1$, up to second order in k, are given in Appendix A.

E. Mean-field limit

The corresponding mean-field dynamics for the Hamiltonian (2) is provided by the discrete nonlinear Schrödinger (DNLS) dimer [22], which in our dimensionless units is given by the system of equations

$$i\frac{dc_1}{d\tau} = -kc_2 + 2(N-1)|c_1|^2 c_1,$$

$$i\frac{dc_2}{d\tau} = -kc_1 + 2(N-1)|c_2|^2 c_2. \tag{14}$$

The complex amplitudes c_1, c_2 satisfy the normalization condition $|c_1|^2+|c_2|^2=1$. This system can be derived either through the Hartree approximation in the time-dependent many-body problem (2) [22], or, equivalently, by the application of the two-mode approximation in the Gross-Pitaevskii equation with a double-well trap [7].

The DNLS dimer is an integrable system and has attracted considerable attention [23–27]. The transfer of many of these results to the problem of a condensate that can tunnel between the minima of a double well has been discussed already [28].

In order to compare the dynamics derived by the mean-field theory (14) with the full quantum problem (12), we calculate the probability difference $|c_2|^2-|c_1|^2$ between the two sites of the DNLS dimer that yields the relative number difference:

$$|c_2|^2-|c_1|^2 \rightarrow \frac{\langle J_z\rangle}{N/2} \tag{15}$$

[see Eq. (6)].

III. COMPLETELY LOCALIZED INITIAL STATES

As a first example we consider the case where all the bosons initially occupy one of the two wells, i.e., $N_2(0)=N$ and $N_1(0)=0$. The corresponding wave function is

$$|\Psi(0)\rangle = \left|\frac{N}{2}\right\rangle. \tag{16}$$

The numerical solution of the quantum system for small values of k, starting with the initial condition (16), displays the following characteristics (see Fig. 1 of Ref. [20]): (i) at short time scales it exhibits small amplitude oscillations around the initial condition, (ii) at longer times, while the bosons still remain localized in the initially occupied trap, collapses and complete revivals appear, and (iii) at even longer times all the atoms coherently tunnel back and forth between the two traps. In Ref. [20] we have presented an analytical expression describing this rich, multiple time-scale dynamics. Below we give the details of this calculation.

A. Short time-scale dynamics

For the moment we disregard the small splittings $\Delta E_{m^\pm}$ of the higher quasidegenerate pairs of levels and we try to find the dominant terms determining the short time-scale evolution. The zeroth-order result of Eq. (12) does not contain any dynamics [29], since only the cross terms n, $n'=(N/2)^\pm$, $(N/2)^\mp$ survive, resulting in

$$\langle J_z^{(0)}(\tau)\rangle = 2Re(\phi^\star_{(N/2)^+}\phi_{(N/2)^-}\langle h_{(N/2)^+}|J_z|h_{(N/2)^-}\rangle) = \frac{N}{2}. \tag{17}$$

To obtain the second equality we have used that in zeroth order $\phi_{(N/2)^\pm}=1/\sqrt{2}$ and the corresponding matrix element from Eq. (A2) is $N/2$.

For the first nonzero time-dependent correction, it is necessary to keep terms up to second order in k in the weights. Then also the cross terms $(N/2)^\pm$, $(N/2-1)^\mp$ and $(N/2-1)^\pm$, $(N/2-1)^\mp$ will contribute to $\langle J_z\rangle$. The first terms will be responsible for the time dependence, providing the characteristic frequency $\omega_\mu=E^{(2)}_{(N/2)^\pm}-E^{(2)}_{(N/2-1)^\pm}$. Using Eq. (9) we obtain that ω_μ, up to second order in k, is given by

$$\omega_\mu = 2(N-1) - k^2 \frac{N+1}{N^2-4N+3}. \tag{18}$$

Taking into account that

$$\phi_{(N/2)^\pm} = \frac{1}{\sqrt{2}}\left(1 - \frac{k^2}{8}\frac{N}{(N-1)^2}\right)$$

[from Eqs. (31) and (32) of Ref. [11] for $m=N/2$],

$$\phi_{(N/2-1)^\pm} = \frac{k}{2\sqrt{2}}\frac{\sqrt{N}}{N-1}$$

[from Eqs. (31) and (33) of Ref. [11] for $m=N/2-1$], and also the relations (A2) and (A4) from Appendix A, we derive that

$$\langle J_z^{(2)}(\tau)\rangle = \frac{N}{2} + \frac{k^2 N}{2(N-1)^2}[\cos(\omega_\mu \tau) - 1]. \tag{19}$$

This equation describes accurately the numerical results at short time scales [see Fig. 1(a) of Ref. [20]]. The calculation of the next order correction in Eq. (19) is also possible. In Appendix B we present this result.

B. Long time-scale dynamics

If we now take into account the splittings $\Delta E_{(N/2)^\pm}$ and $\Delta E_{(N/2-1)^\pm}$ of the two higher pairs of quasidegenerate energy levels, they affect the evolution on longer time scales. The former will appear already in the zeroth-order result (17) and will describe complete transfer of all the bosons back and forth between the two equivalent traps. The latter will appear at second order, not only in the cross terms $(N/2-1)^\pm, (N/2-1)^\mp$, but also in the sum of the terms $(N/2)^\pm$ and $(N/2-1)^\mp$, providing the beat that gives rise to the observed collapses and revivals. In the latter case the difference of the energies $E_{(N/2)^+} - E_{(N/2-1)^-}$ and $E_{(N/2)^-} - E_{(N/2-1)^+}$ will be equal to $\Delta E_{(N/2-1)^\pm}$ at a lower order in k. Repeating the calculations as in the preceding section, we find the result presented in Eq. (3) of Ref. [20]:

$$\langle J_z^{(2)}(\tau)\rangle = \frac{N}{2}\cos(\omega_0\tau) + \frac{k^2 N}{4(N-1)^2}\left[\frac{N}{2}[\cos(\omega_1\tau) - \cos(\omega_0\tau)] + 2\cos(\omega_\mu\tau)\cos\left(\frac{\omega_1}{2}\tau\right) - \cos(\omega_1\tau) - \cos(\omega_0\tau)\right]. \tag{20}$$

For $\omega_0 = 0$ and $\omega_1 = 0$, Eq. (20) gives the result (19) for short time scales. In the last expression the frequencies ω_0 and ω_1 correspond to the splittings $\Delta E_{(N/2)^\pm}$ and $\Delta E_{(N/2-1)^\pm}$ of the two higher quasidegenerate energy pairs, respectively, which are given by [20]

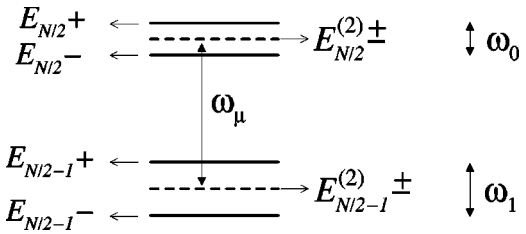

FIG. 1. Schematic of the two upper quasidegenerate pairs of energy levels. Up to second order in k they are still degenerate with energies $E^{(2)}_{(N/2)^\pm}$ and $E^{(2)}_{(N/2-1)^\pm}$, respectively. This energy difference provides the short time-scale oscillating frequency ω_μ. At higher order in k these quasidegenerate pairs split, providing the frequencies ω_1 and ω_0 that characterize the collapses/revivals and the coherent tunneling between the two sites, respectively. The sketch refers to the case of even N. For odd N the levels $E_{(N/2)^-}$ and $E_{(N/2-1)^-}$ will be higher in energy than $E_{(N/2)^+}$ and $E_{(N/2-1)^+}$, respectively.

$$\omega_0 = \Delta E_{(N/2)^\pm} = k^N \frac{N}{2^{N-2}(N-1)!} \tag{21}$$

and

$$\omega_1 = \Delta E_{(N/2-1)^\pm} = k^{N-2}\frac{(N-1)(N-2)}{2^{N-4}(N-3)!}. \tag{22}$$

In Fig. 1 we present the relevant part of the energy spectrum that is responsible for the dynamics exhibited by a completely localized initial state at small values of tunneling amplitude.

C. Comparison with the mean-field dynamics

For completely localized initial conditions the solutions of the integrable DNLS dimer are given in terms of the Jacobian elliptic functions [23,25,26]. In particular, appropriate for our discussion is the region where $(N-1)/2k > 1$. In that case we are in the self-trapped regime and the solution of Eq. (14) is obtained through [25]

$$|c_2|^2 - |c_1|^2 = \frac{N_2 - N_1}{N} = dn\left((N-1)\tau; \frac{2k}{N-1}\right), \tag{23}$$

where $2k/(N-1)$ is the modulus κ of the Jacobian elliptic function $dn(u;\kappa)$ [30]. For very small κ, the expansion $dn(u;\kappa) = 1 - (\kappa^2/2)\sin^2(u)$ in Eq. (23) yields that

$$\frac{N_2 - N_1}{N} = 1 - \frac{2k^2}{(N-1)^2}\sin^2[(N-1)\tau]. \tag{24}$$

[See also Eq. (9) of Ref. [25], where V and χ of that reference correspond to $-k$ and $-2(N-1)$, respectively.] Taking into account Eq. (6) we see that the last expression is identical with the perturbative result (19), using the zeroth-order term for the frequency ω_μ, Eq. (18). We find that in the limit of small tunneling amplitude the mean-field dynamics accurately provides the short time-scale evolution. How-

ever, it is unable to account for the richer behavior on longer time scales, namely, collapses and revivals, as well as coherent tunneling [20].

IV. COHERENT SPIN INITIAL STATES: SHORT TIME-SCALE DYNAMICS

The second initial condition that we consider consists of the coherent spin states (or the angular momentum coherent states) [31,32] that, in analogy with the usual harmonic oscillator coherent states, provide an analogous quantum description with the corresponding classical angular momenta. Such initial conditions have also been used in Ref. [9]. A coherent spin state is characterized by two angles θ and ϕ (similar to the case of a classical angular momentum with fixed magnitude) and is obtained by

$$|\Psi(0)\rangle = C \sum_{m=-N/2}^{N/2} \sqrt{\frac{N!}{\left(\frac{N}{2}+m\right)!\left(\frac{N}{2}-m\right)!}} \times \tan^m\left(\frac{\theta}{2}\right) e^{-im\phi}|m\rangle, \tag{25}$$

where the coefficient C is given by

$$C = \sin^{N/2}\left(\frac{\theta}{2}\right)\cos^{N/2}\left(\frac{\theta}{2}\right)e^{-i(N/2)\phi}. \tag{26}$$

For the initial state of Eq. (25) we have that

$$\langle\Psi(0)|J_z|\Psi(0)\rangle = -\frac{N}{2}\cos(\theta). \tag{27}$$

We will consider only the dynamics on short time scales and then we ignore in the following part of the section the splittings of the quasidegenerate pairs that are obtained in higher order than k^2.

A. Dominant frequency

If we keep zeroth-order terms in Eq. (12) and we take into account the results of Appendix A, it is obvious that the time dependence will be obtained through the splittings $\Delta E_{1^\pm}$ and $\Delta E_{1/2^\pm}$ of Eqs. (11) and (10) for even and odd N, respectively. We present separately the results for these two cases.

1. Even N

Calculating the corresponding $\phi_{n^\pm}$ for the initial state (25) in zeroth order and using Eqs. (27) and (A2), we obtain from Eq. (12) that

$$\langle J_z^{(0)}(\tau)\rangle = -\frac{N}{2}\cos(\theta) + \left(\frac{\sin(\theta)}{2}\right)^N \frac{N!}{\left(\frac{N}{2}+1\right)!\left(\frac{N}{2}-1\right)!}\left\{\left[\tan^2\left(\frac{\theta}{2}\right) - \frac{1}{\tan^2\left(\frac{\theta}{2}\right)}\right][\cos(\omega_e\tau)-1] + 2\sin(2\phi)\sin(\omega_e\tau)\right\}, \tag{28}$$

where the frequency ω_e is given by

$$\omega_e = E_{1^+} - E_{1^-} = k^2\frac{N}{2}\left(\frac{N}{2}+1\right). \tag{29}$$

2. Odd N

In this case Eq. (12) similarly yields in zeroth order

$$\langle J_z^{(0)}(\tau)\rangle = -\frac{N}{2}\cos(\theta) + \frac{1}{2}\left(\frac{\sin(\theta)}{2}\right)^N \frac{N!}{\left(\frac{N}{2}+\frac{1}{2}\right)!\left(\frac{N}{2}-\frac{1}{2}\right)!} \times \left\{\left[\tan\left(\frac{\theta}{2}\right) - \frac{1}{\tan\left(\frac{\theta}{2}\right)}\right][\cos(\omega_e\tau)-1] - 2\sin(\phi)\sin(\omega_e\tau)\right\}, \tag{30}$$

where now ω_e is obtained by

$$\omega_e = E_{1/2^-} - E_{1/2^+} = 2k\sqrt{\frac{N}{2}\left(\frac{N}{2}+1\right)+\frac{1}{4}}. \tag{31}$$

In Figs. 2 and 3 we show with red lines the harmonic expressions (28) and (30) for two coherent states and for different number N of bosons. By comparing with the corresponding numerical results (black lines) we see that the zeroth-order perturbative results provide the dominant frequency of the short time-scale evolution. We note in Figs. 2 and 3 the significant differences in the periods of the corresponding dominant oscillations between odd [Figs. 2(a,c,e) and 3(a,c,e)] and even N [Figs. 2(b,d,f) and 3(b,d,f)]. This is due to the fact that the frequency ω_e is of first, Eq. (31), and second order, Eq. (29), in k, respectively.

B. Manifestation of the whole energy spectrum

Although the analytical results (28) and (30) give the dominant frequency, they are not able to describe the fluctuations exhibited by the numerical results. These fluctuations become stronger as N increases. In order to account for them, it is necessary to keep up to first-order terms in Eq. (12). Using the results (A2)–(A5) from Appendix A and the

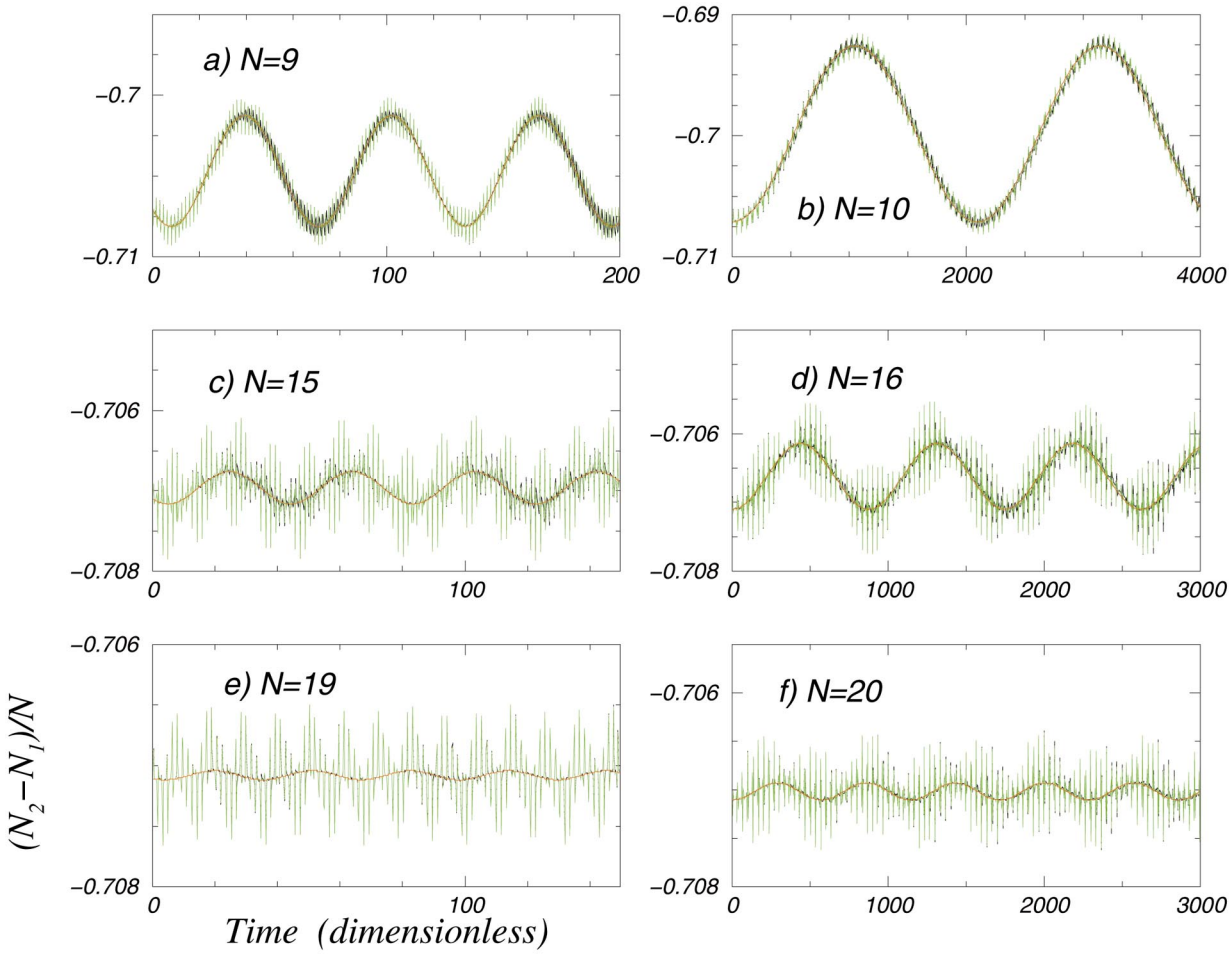

FIG. 2. (Color) Time evolution of the relative atom number difference, $2\langle J_z\rangle/N$, between the two sites of the double well for a coherent initial state with $\theta=\pi/4$ and $\phi=\pi/2$, in a system consisting of (a) $N=9$, (b) $N=10$, (c) $N=15$, (d) $N=16$, (e) $N=19$, and (f) $N=20$ bosons. The dimensionless tunneling amplitude is $k=0.01$. The black lines represent numerical results, the red lines represent zeroth-order analytical results given by Eq. (28) [Eq. (30)], and the green lines represent first-order analytical results provided by Eqs. (32), (33), and (35)–(37) [Eqs. (38)–(40)] for even (odd) N.

$\phi_{n^\pm}$ for the initial state (25) up to first order [from Eqs. (31) and (33) of Ref. [11]], after some straightforward calculations Eq. (12) yields

$$\langle J_z^{(1)}(\tau)\rangle=\langle J_z^{(0)}(\tau)\rangle+k\left(\frac{\sin(\theta)}{2}\right)^N \times\Bigg[C_1[\cos(\omega_e\tau)-1]+C_2\sin(\omega_e\tau) +\sum_{n=0or1/2}^{N/2-1}\frac{N!}{\left(\frac{N}{2}+n\right)!\left(\frac{N}{2}-n\right)!}\frac{N-2n}{2(2n+1)}A_n\Bigg], \tag{32}$$

where

$$A_n=\tan^{2n+1}\left(\frac{\theta}{2}\right)[\cos(F_n\tau+\phi)-\cos(\phi)] -\frac{1}{\tan^{2n+1}\left(\frac{\theta}{2}\right)}[\cos(F_n\tau-\phi)-\cos(\phi)]. \tag{33}$$

In Eq. (32) apart from the dominant frequency ω_e, time dependence results also through the quantities A_n appearing in the sum of the last term. The corresponding frequencies of Eq. (33), F_n, are given through the differences of the adjacent quasidegenerate pairs of levels, as

$$F_n=E_{(n+1)^\pm}-E_{(n)^\mp}=4n+2, \tag{34}$$

where in obtaining the last equality we have used the lower-order result in k, Eq. (7). The fine structure of these levels, i.e., the difference between the terms $E_{(n+1)^+}-E_{(n)^-}$ and $E_{(n+1)^-}-E_{(n)^+}$ will be manifested at later times and do not

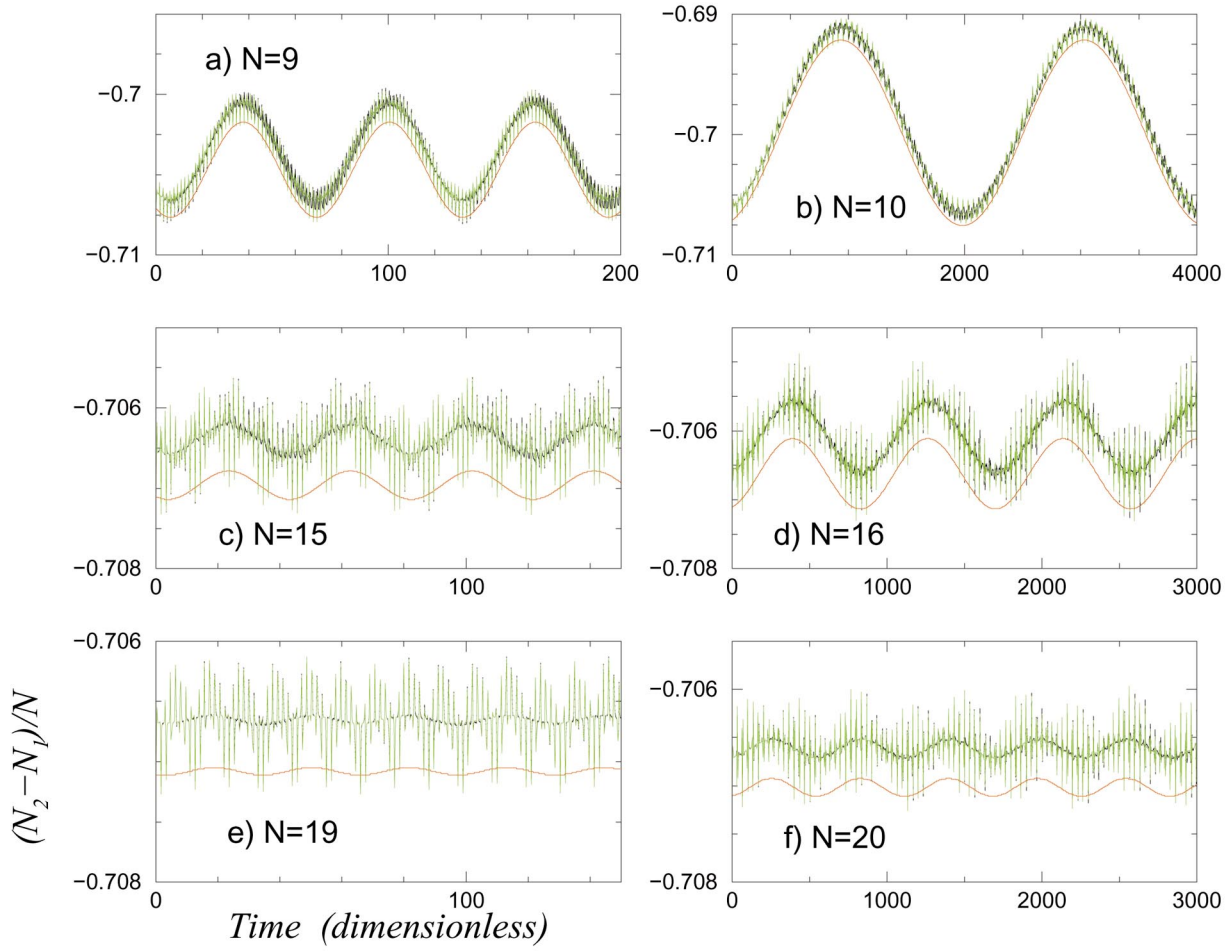

FIG. 3. (Color) Time evolution of the relative atom number difference, $2\langle J_z\rangle/N$, between the two sites of the double well for a coherent initial state with $\theta=\pi/4$ and $\phi=\pi/4$, in a system consisting of (a) $N=9$, (b) $N=10$, (c) $N=15$, (d) $N=16$, (e) $N=19$, and (f) $N=20$ bosons. The dimensionless tunneling amplitude is $k=0.01$. The black lines represent numerical results, the red lines represent zeroth-order analytical results given by Eq. (28) [Eq. (30)], and the green lines represent first-order analytical results provided by Eqs. (32), (33), and (35)–(37) [Eqs. (38)–(40)] for even (odd) N.

affect the short time-scale dynamics. This effect appears earlier in the cases of odd N through the terms $F_{1/2}$.

1. Even N

For an even number of bosons, the coefficients C_1 and C_2 that appear in Eq. (32) are

$$C_1=\frac{N!}{\left(\frac{N}{2}+1\right)!\left(\frac{N}{2}-1\right)!}\cos(\phi)\left\{\left(\frac{N}{6}-\frac{1}{3}\right)\left[\tan^3\left(\frac{\theta}{2}\right)-\frac{1}{\tan^3\left(\frac{\theta}{2}\right)}\right]-\left(\frac{N}{2}+1\right)\left[\tan\left(\frac{\theta}{2}\right)-\frac{1}{\tan\left(\frac{\theta}{2}\right)}\right]\right\}, \tag{35}$$

$$C_2=\frac{N!}{\left(\frac{N}{2}+1\right)!\left(\frac{N}{2}-1\right)!}\left[\tan\left(\frac{\theta}{2}\right)+\frac{1}{\tan\left(\frac{\theta}{2}\right)}\right]\times\left[\left(\frac{N}{6}-\frac{1}{3}\right)\sin(3\phi)-\left(\frac{N}{2}+1\right)\sin(\phi)\right], \tag{36}$$

and the frequencies F_n appearing in the sum of Eq. (32) are given by

$$F_n=4n+2,\quad n=0,1,\ldots,\frac{N}{2}-1\Rightarrow F_n=2,6,10,\ldots,2N-2. \tag{37}$$

2. Odd N

In the case of an odd number of bosons, the corresponding coefficients are given by

$$C_1=\frac{N!}{\left(\frac{N}{2}+\frac{1}{2}\right)!\left(\frac{N}{2}-\frac{1}{2}\right)!}\frac{N-1}{8}\cos(\phi)$$

$$\times\left[\tan^2\left(\frac{\theta}{2}\right)-\frac{1}{\tan^2\left(\frac{\theta}{2}\right)}\right], \quad (38)$$

$$C_2=\frac{N!}{\left(\frac{N}{2}+\frac{1}{2}\right)!\left(\frac{N}{2}-\frac{1}{2}\right)!}\frac{N-1}{8}\sin(2\phi)$$

$$\times\left[\tan\left(\frac{\theta}{2}\right)+\frac{1}{\tan\left(\frac{\theta}{2}\right)}\right], \quad (39)$$

and the frequencies F_n of Eq. (33) are

$$F_n=4n+2,$$

$$n=\frac{1}{2},\frac{3}{2},\ldots,\frac{N}{2}-1\Rightarrow F_n=4,8,12,\ldots,2N-2. \quad (40)$$

The green lines in Figs. 2 and 3 show the analytical expressions (32)–(34) together with Eqs. (35) and (36) for even N, and Eqs. (38) and (39) for odd N. We see that they accurately provide the quantum fluctuations of the numerical solutions, since the two evolutions cannot be distinguished on the presented time scales.

In Fig. 4 we demonstrate the Fourier transform of the numerical solutions of Figs. 2(e) and 2(f) for the case of an odd and an even number of bosons, respectively. The resulting frequencies are in agreement with the calculated values in Eqs. (40) and (37), respectively. Also in Fig. 4(a) the splitting of the frequency $F_{1/2}=4$ appears weakly, in accordance with the discussion following Eq. (34). In the insets we show the regime close to zero, where the low frequencies ω_e appear. The corresponding result for the case of Fig. 4(a) [Fig. 4(b)], as obtained through Eq. (31) [Eq. (29)], is $\omega_e=0.2$ ($\omega_e=0.011$).

C. Comparison with the mean-field dynamics

The evolution of the quantity $|c_2|^2-|c_1|^2$ obeying Eq. (14) for an arbitrary initial condition is equivalent to the trajectory of a particle moving in the potential $D_1x^4+D_2x^2$, where the coefficients D_1 and D_2 depend on the initial condition [25,26]. D_1 is always positive, while D_2 may be positive or negative. The initial position and the velocity of the particle are given by the quantities $|c_2|^2-|c_1|^2$ and $i2k(c_2^\star c_1-c_1c_2^\star)$, respectively, evaluated at $\tau=0$ [26]. In any case the solution is periodic containing a single frequency and its harmonics. Such a solution cannot describe the irregular quantum dynamics exhibited in Figs. 2 and 3.

In Fig. 5 we show the mean-field solutions for some cases presented in Fig. 2. We have used the same scale in the y axis with the corresponding plots of Fig. 2 in order to compare

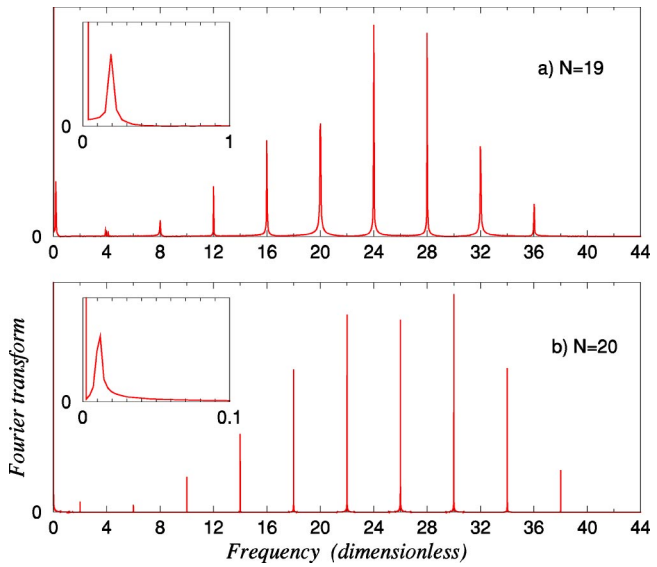

FIG. 4. (Color online) Fourier transform of the numerical evolution of the relative atom number difference, $2\langle J_z\rangle/N$, between the two sites of the double well for a coherent initial state with $\theta=\pi/4$ and $\phi=\pi/2$, in a system consisting of (a) $N=19$ and (b) $N=20$ bosons [cases demonstrated in Figs. 2(e) and 2(f), respectively]. The dimensionless tunneling amplitude is $k=0.01$. We observe the appearance of the characteristic frequencies F_n, provided by Eq. (37) for even N and Eq. (40) for odd N, respectively. The insets show a magnification of the spectra close to zero, where the low frequencies ω_e, Eqs. (29) and (31), respectively, appear.

the results. The mean-field frequency does not coincide with the dominant frequency of the quantum evolution. It is rather in the region of the higher frequencies appearing in the first-order corrections. We note that the amplitude of the mean-field oscillations vary in a similar way to the amplitude of the quantum fluctuations. As a result, for larger N, where the quantum fluctuations gradually suppress the dominant frequency (see Figs. 2 and 3), the DNLS solution improves its agreement with the quantum solution.

We can obtain some analytical results for the mean-field evolution of the relative number difference in the small k regime. The relevant initial conditions for the DNLS dimer that correspond to a coherent spin state are

$$c_1(\tau=0)=\sqrt{\frac{1-z}{2}},\quad c_2(\tau=0)=\sqrt{\frac{1+z}{2}}e^{i\phi}, \quad (41)$$

where $z=-\cos(\theta)=(|c_2|^2-|c_1|^2)$ $(\tau=0)$. In the equivalent picture of a particle moving in the potential $V(x)=D_1x^4+D_2x^2$, its mass is unity and the position of the particle gives the relative number difference $|c_2|^2-|c_1|^2$. The potential in our notation is given by [25,26]

$$V(x)=\frac{(N-1)^2}{2}x^4+[-(N-1)^2\cos^2(\theta)+4k^2$$

$$+4k(N-1)\sin(\theta)\cos(\phi)]x^2. \quad (42)$$

Since $k/(N-1)\ll 1$ in our case, it suffices to retain the first term in the coefficient of x^2 for most of the following calcu-

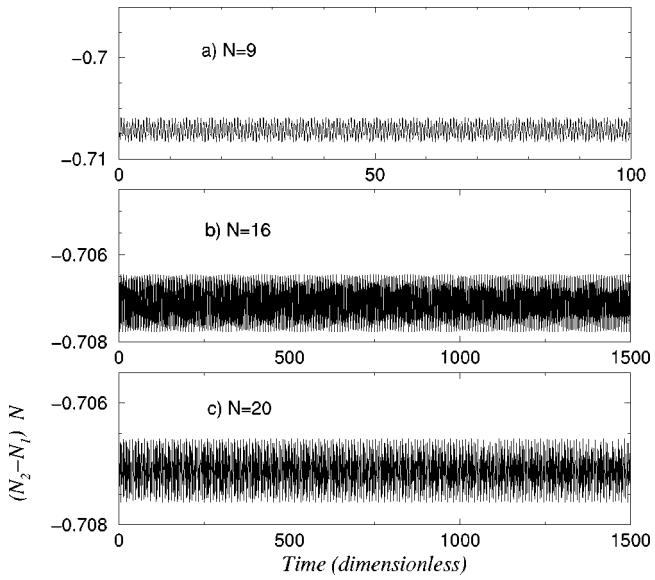

FIG. 5. Time evolution of the relative atom number difference, $|c_2|^2-|c_1|^2$, in the mean-field approximation for a coherent initial state with $\theta=\pi/4$ and $\phi=\pi/2$, in a system consisting of (a) $N=9$, (b) $N=16$, and (c) $N=20$ bosons [cases demonstrated in Figs. 2(a), 2(d), and 2(f), respectively]. The dimensionless tunneling amplitude is $k=0.01$. In all the cases the dynamics is nearly harmonic.

lations. The corresponding initial conditions for the particle are given by [26] $x(\tau=0)=-\cos(\theta)$ and $dx/dt(\tau=0)=2k\sin(\theta)\sin(\phi)$. The double-well potential $V(x)$ (that should not be confused with the trap of the bosons) has a local maximum at $x=0$ and two symmetric minima at $x=\pm\cos(\theta)+o[k/(N-1)]$. Initially the particle is very close to the minimum x_0 around $-\cos(\theta)$, at a distance of the order $k/(N-1)$, and has a nonzero velocity of order k. As a result its time evolution is a small amplitude oscillation that can be obtained by linearizing the potential around its minimum at x_0, i.e.,

$$\frac{N_2-N_1}{N}=\Pi\cos(\omega_{mf}\tau+\psi_0), \tag{43}$$

where ψ_0 is an initial phase. The single frequency of the mean-field dynamics is obtained by

$$\omega_{mf}=2(N-1)\cos(\theta), \tag{44}$$

where the next correction is of order $k/(N-1)$. The maximum amplitude Π of the oscillation is obtained through the relation

$$\frac{1}{2}\left(\frac{dx}{dt}(\tau=0)\right)^2+\frac{1}{2}\omega_{mf}^2[x(\tau=0)-x_0]^2=\frac{1}{2}\omega_{mf}^2\Pi^2,$$

which yields in lowest order

$$\Pi=\frac{k}{N-1}\tan(\theta)\sqrt{3\cos^2(\phi)+1}. \tag{45}$$

In deriving the last equation we have used the first correction in x_0, which is $[2k/(N-1)]\tan(\theta)\cos(\phi)$.

The relations (44) and (45) are in a very good agreement with the numerical solutions presented in Fig. 5. We see that the mean-field single frequency, Eq. (44), lies in between the zeroth-order frequencies F_n of Eqs. (37) and (40) and its actual position is determined by the angle θ of the coherent initial state. For example, in the case displayed in Fig. 5(c), $\omega_{mf}\approx 26.9$, while for the same initial condition and $N=19$, $\omega_{mf}\approx 25.5$. One can compare these frequencies with the corresponding quantum spectra of Figs. 4(b) and 4(a), respectively.

V. CONCLUSIONS

By applying results obtained from perturbation theory for the stationary states of the boson-Hubbard dimer in the small tunneling amplitude regime, we have derived analytical expressions for the time evolution of the number difference of bosons between the two equivalent sites. The obtained formulas account well for the complex quantum evolution of the system.

In the case that all the bosons initially occupy one trap of the potential, the numerical solution exhibits a rich behavior on different time scales. This multiple time-scale dynamics is determined by the structure of the upper part of the energy spectrum; the two higher quasidegenerate pairs of levels. The difference between these two quasidegenerate pairs, which is zeroth order in k, is responsible for the small amplitude oscillations on short time scales. The small splitting of the second higher pair, of the order k^{N-2}, determines at longer times the collapses and revivals that correspond to the vanishing and the subsequent complete restoration of the oscillation amplitude. Up to this point the bosons remain localized in the initially occupied site. Then, at even longer time scales, the very small splitting of the higher pair of levels, of the order k^N, gives rise to coherent tunneling at the initially unoccupied trap of the potential. The corresponding mean-field dynamics is identical with the short time-scale evolution but fails to reproduce different behavior observed at larger time scales. Collapses and revivals that contrast the mean-field results have been observed in this context in Ref. [7]. These characteristic signatures of quantum evolution have also been studied in quantum optics [33–35]. Furthermore, the complete transfer of all the bosons between the two traps of the boson-Hubbard dimer, as a pure quantum effect for small tunneling amplitudes, has been nicely discussed in Refs. [14,15]. With increasing N the periods of the quantum features are strongly increased, resulting in the validity of the mean-field description at much longer times [9,14].

The initial condition of a coherent spin state reveals more irregular dynamics, with quantum fluctuations that increase with the number of bosons. The dominant frequency in this evolution is obtained by the larger splitting occurring at the unperturbed degenerate pairs. This is determined by the lower part of the spectrum; for an odd number of bosons it is the difference between the ground and the first excited states, while for even N it is the splitting between the first and the second excited states. Apart from this low frequency, of order k, or k^2, depending on whether N is odd or even, respectively, the whole spectrum is manifested on short time scales

through the exhibited fluctuations. The latter are provided by the differences of adjacent quasidegenerate levels, which are of zeroth order in k. The mean-field dynamics is obviously unable to describe the quantum fluctuations, yielding a single oscillation. Its period is much smaller than that of the dominant frequency appearing in the quantum dynamics. Nevertheless, as the number of bosons is increased, it more closely mimics the quantum evolution.

The demonstration of a BEC trapped in a double-well potential has been experimentally achieved in Ref. [12]. By focusing a far off-resonant laser beam at the center of a magnetic trap in this experiment, a repulsive optical force is produced, which separates the sodium atom condensate into two symmetric wells. Furthermore, these authors were able to create a situation in which all the atoms of the BEC were localized at one minimum of the double well, by illuminating—using weak resonant light—the other trap and pumping its atoms to untrapped states (see Fig. 1(b) of Ref. [12]). We note that the presented results for the boson-Hubbard dimer are not applicable in the situation of this experiment due to the large number of the trapped bosons (of the order of millions). However, condensates with a few thousands of atoms have been realized [3], and the creation of barriers in these cases would provide a realistic situation for the application of the two-mode approximation.

ACKNOWLEDGMENTS

We acknowledge stimulating discussions with K. Ø. Rasmussen. This research was supported by the U.S. Department of Energy under Contract No. W-7405-ENG-36, the NSF under Grant No. DMR0097204, and a contract from LANL to the University of New Mexico's Consortium of the Americas.

APPENDIX A

In general, for each pair of n, $n'=0$ or $1/2,\ldots,N/2$ is

$$\langle h_{n^+}|J_z|h_{n'^+}\rangle=0=\langle h_{n^-}|J_z|h_{n'^-}\rangle. \tag{A1}$$

As a result only cross terms of different symmetry survive in the double sum of Eq. (12).

Using the relations (27)–(34) of Ref. [11] we obtain the following results up to second order in k. For $n'=n$,

$$\langle h_{n^\pm}|J_z|h_{n^\mp}\rangle=n\left(1-\frac{k^2}{2}\frac{4J^2n^2+J^2-4n^4+3n^2}{(4n^2-1)^2}\right)+\frac{k^2}{4}\left(\frac{J^2-n(n+1)}{(2n+1)^2}(n+1)+\frac{J^2-n(n-1)}{(2n-1)^2}(n-1)\right)\quad \text{for } n\geqslant 1 \tag{A2}$$

and

$$\langle h_{1/2^\pm}|J_z|h_{1/2^\mp}\rangle=\frac{1}{2}+\frac{k^2}{16}(J^2-1), \tag{A3}$$

while for $n'=n+1$

$$\langle h_{n^\pm}|J_z|h_{(n+1)^\mp}\rangle=\frac{k}{2}\frac{\sqrt{J^2-n(n+1)}}{2n+1}\quad \text{for } n>0 \tag{A4}$$

and

$$\langle h_0|J_z|h_{1^-}\rangle=k\sqrt{\frac{J^2}{2}}. \tag{A5}$$

The matrix elements $\langle h_{n^\pm}|J_z|h_{(n-1)^\mp}\rangle$ for $n>1$ are obtained by substituting $n=n-1$ in the expression (A4).

The general matrix elements $\langle h_{n^\pm}|J_z|h_{(n+2)^\mp}\rangle$ and $\langle h_{n^\pm}|J_z|h_{(n-2)^\mp}\rangle$ are of order k^2, but we do not use them in the text. All other matrix elements are zero up to second order in k.

APPENDIX B

The next order correction in the result of Eq. (19) contains the term

$$-\frac{k^4N}{8(N-2)(N-3)^2}\left(\frac{N^4-8N^3+22N^2-8N-23}{(N-1)^4}[\cos(\omega_\mu\tau)-1]-[\cos(\omega_{\mu''}\tau)-1]-\frac{1}{N-2}[\cos(\omega_{\mu'}\tau)-1]\right), \tag{B1}$$

where the frequency ω_μ is given by Eq. (18), and $\omega_{\mu'}$ and $\omega_{\mu''}$ are given by $E^{(2)}_{(N/2)^\pm}-E^{(2)}_{(N/2-2)^\pm}$ and $E^{(2)}_{(N/2-1)^\pm}-E^{(2)}_{(N/2-2)^\pm}$, respectively. The corresponding results, up to second order in k, are

$$\omega_{\mu'}=4(N-2)-2k^2\frac{N^2-N-2}{N^3-9N^2+23N-15} \tag{B2}$$

and

$$\omega_{\mu''}=2(N-3)-k^2\frac{N^3-N^2-5N-3}{N^4-12N^3+50N^2-84N+45}. \tag{B3}$$

In order to calculate the term (B1), we have used the relations (31)–(34) of Ref. [11] for $m=N/2$, $N/2-1$, and $N/2-2$. Moreover, it is necessary to calculate for the eigenvector $|h_{(N/2)^\pm}\rangle$ the third order correction in the coefficient of $|(N/2-1)^\mp\rangle$, equal to

$$\frac{k^3}{16}\frac{\sqrt{N}(N^2-2N-2)}{(N-1)^3(N-2)},$$

and the fourth-order correction in the coefficient of $|(N/2)^{\pm}\rangle$, which is

$$\frac{k^4}{128}\frac{N(N^3-6N^2-2N-18)}{(N-1)^4(N-2)^2},$$

as well as for the eigenvector $|h_{(N/2-1)^{\pm}}\rangle$ the third-order correction in the coefficient of $|(N/2)^{\pm}\rangle$, equal to

$$-\frac{k^3}{16\sqrt{2}}\frac{\sqrt{N}(N^3-4N^2+5N+10)}{(N-1)^3(N-3)^2}.$$

The correction (B1) is appropriate for small time scales, since we have not taken into account the small splittings $\Delta E_{(N/2)^{\pm}}$, $\Delta E_{(N/2-1)^{\pm}}$, and $\Delta E_{(N/2-2)^{\pm}}$, of order k^N, k^{N-2}, and k^{N-4}, respectively.

[1] E.P. Gross, Nuovo Cimento **20**, 454 (1961); J. Math. Phys. **4**, 195 (1963).
[2] L.P. Pitaevskii, Sov. Phys. JETP **13**, 451 (1961).
[3] F. Dalfovo, S. Giorgini, L.P. Pitaevskii, and S. Stringari, Rev. Mod. Phys. **71**, 463 (1999).
[4] J. Denschlag *et al.*, Science **287**, 97 (2000); B.P. Anderson *et al.*, Phys. Rev. Lett. **86**, 2926 (2001).
[5] C. Orzel *et al.*, Science **291**, 2386 (2001).
[6] A. Tuchman *et al.* (unpublished).
[7] G.J. Milburn, J. Corney, E.M. Wright, and D.F. Walls, Phys. Rev. A **55**, 4318 (1997).
[8] M.J. Steel and M.J. Collett, Phys. Rev. A **57**, 2920 (1998).
[9] S. Raghavan, A. Smerzi, and V.M. Kenkre, Phys. Rev. A **60**, R1787 (1999).
[10] J. Javanainen and M.Y. Ivanov, Phys. Rev. A **60**, 2351 (1999).
[11] G. Kalosakas and A.R. Bishop, Phys. Rev. A **65**, 043616 (2002).
[12] M.R. Andrews *et al.*, Science **275**, 637 (1997).
[13] A.C. Scott and J.C. Eilbeck, Phys. Lett. A **119**, 60 (1986).
[14] L. Bernstein, J.C. Eilbeck, and A.C. Scott, Nonlinearity **3**, 293 (1990).
[15] L. Bernstein, Physica D **68**, 174 (1993).
[16] D.S. Hall, M.R. Matthews, J.R. Ensher, C.E. Wieman, and E.A. Cornell, Phys. Rev. Lett. **81**, 1539 (1998).
[17] J. Williams, R. Walser, J. Cooper, E. Cornell, and M. Holland, Phys. Rev. A **59**, R31 (1999).
[18] J.M. Vogels *et al.*, Phys. Rev. A **56**, R1067 (1997).
[19] S. Inouye *et al.*, Nature (London) **392**, 151 (1998).
[20] G. Kalosakas, A.R. Bishop, and V.M. Kenkre, J. Phys. B: At. Mol. Opt. Phys. **36**, 3233 (2003).
[21] C. Cohen-Tannoudji, B. Diu, and F. Laloe, *Quantum Mechanics* (Wiley-Interscience, Paris, 1977) Vol. I; L.D. Landau and E.M. Lifshitz, *Quantum Mechanics, Non-relativistic Theory* (Pergamon Press, London, 1958).
[22] E. Wright, J.C. Eilbeck, M.H. Hays, P.D. Miller, and A.C. Scott, Physica D **69**, 18 (1993).
[23] A.A. Maier, Sov. J. Quantum Electron. **14**, 101 (1984).
[24] J.C. Eilbeck, P.S. Lomdahl and A.C. Scott, Physica D **16**, 318 (1985); J.C. Eilbeck, in *Davydov's Soliton Revisited*, edited by P.L. Christiansen and A.C. Scott (Plenum Press, New York, 1990), p. 473.
[25] V.M. Kenkre and D.K. Campbell, Phys. Rev. B **34**, R4959 (1986).
[26] V.M. Kenkre and G.P. Tsironis, Phys. Rev. B **35**, 1473 (1987).
[27] G.P. Tsironis and V.M. Kenkre, Phys. Lett. A **127**, 209 (1988).
[28] S. Raghavan, A. Smerzi, S. Fantoni, and S.R. Shenoy, Phys. Rev. A **59**, 620 (1999).
[29] We consider $N>4$ in our discussion.
[30] P.F. Byrd and M.D. Friedman, *Handbook of Elliptic Integrals for Engineers and Scientists* (Springer-Verlag, Berlin, 1971).
[31] J.M. Radcliffe, J. Phys. A **4**, 313 (1971).
[32] F.T. Arecchi, E. Courtens, R. Gilmore, and H. Thomas, Phys. Rev. A **6**, 2211 (1972).
[33] N.B. Narozhny, J.J. Sanchez-Mondragon, and J.H. Eberly, Phys. Rev. A **23**, 236 (1981).
[34] P. Alsing and M.S. Zubairy, J. Opt. Soc. Am. B **4**, 177 (1987).
[35] D.A. Cardimona *et al.*, Phys. Rev. A **43**, 3710 (1991); D.A. Cardimona, V. Kovanis, and M.P. Sharma, *ibid.* **47**, 1227 (1993).